Cancer Cell
Article

Genes that Distinguish Physiological and Pathological Angiogenesis

Steven Seaman,[1] Janine Stevens,[1] Mi Young Yang,[1] Daniel Logsdon,[2] Cari Graff-Cherry,[2] and Brad St. Croix[1,*]
[1] Tumor Angiogenesis Section, Mouse Cancer Genetics Program
[2] Basic Research Program, SAIC
National Cancer Institute at Frederick, Frederick, MD 21702, USA
*Correspondence: stcroix@ncifcrf.gov
DOI 10.1016/j.ccr.2007.04.017

SUMMARY

To unravel the normal vasculature transcriptome and determine how it is altered by neighboring malignant cells, we compared gene expression patterns of endothelial cells derived from the blood vessels of eight normal resting tissues, five tumors, and regenerating liver. Organ-specific endothelial genes were readily identified, including 27 from brain. We also identified 25 transcripts overexpressed in tumor versus normal endothelium, including 13 that were not found in the angiogenic endothelium of regenerating liver. Most of the shared angiogenesis genes have expected roles in cell-cycle control, but those specific for tumor endothelium were primarily cell surface molecules of uncertain function. These studies reveal striking differences between physiological and pathological angiogenesis potentially important for the development of tumor-specific, vascular-targeted therapies.

INTRODUCTION

Angiogenesis is required for the progression of many diseases, including age-related macular degeneration and cancer (Kerbel and Folkman, 2002; Ferrara and Kerbel, 2005). Inhibiting or destroying abnormal blood vessels associated with cancer and other diseases using either antiangiogenic agents or vascular disrupting agents has become a major therapeutic strategy. However, angiogenesis is also required for normal physiological processes, such as corpus luteum formation in the ovary and endometrial regeneration during the menstrual cycle. Current targets of antiangiogenic therapy, such as VEGF, are thought to be critical for both physiological and pathological angiogenesis, and clinical side effects of anti-VEGF therapy are beginning to emerge. Cross-reactivity with normal tissues is even more of a concern for the development of vascular disrupting agents, i.e., cytotoxic drugs that target newly formed blood vessels. Thus, markers that can separate physiological and pathological angiogenesis are urgently needed in order to selectively deliver antiangiogenic or vascular disrupting agents to diseased tissues, minimizing the potential for side effects. In an attempt to identify targets on the endothelial cells (ECs) that line tumor blood vessels, we previously compared gene expression patterns in ECs derived from either normal or malignant colorectal tissues. These studies led to the identification of 46 tumor endothelial markers, called TEMs (St. Croix et al., 2000). Further studies on a subset of these (TEM1–TEM9) revealed that each of them, with the possible exception of TEM8, are also elevated in the vessels of the corpus luteum during physiological angiogenesis (St. Croix et al., 2000; Nanda et al., 2004). The identification of TEM8 suggests that markers with an expression pattern more restricted to tumor vessels may exist. However, which

SIGNIFICANCE

Angiogenesis is critical for the progression of many diseases, including age-related macular degeneration and cancer. Markers that can separate physiological and pathological angiogenesis are urgently needed in order to selectively deliver antiangiogenic or vascular disrupting agents to diseased tissues, minimizing the potential for side effects. By comparing the vascular transcriptome of normal resting, normal proliferating, and malignant tissues, we have identified several genes that are selectively overexpressed on blood vessels during tumor angiogenesis. These studies reveal striking differences between physiological and pathological angiogenesis at the molecular level and provide potential targets to guide the selective delivery of molecular agents to specific anatomical sites, including cancer.

genes and how many share this pattern are important unanswered questions.

What factors might influence gene expression during tumor angiogenesis but not normal physiological angiogenesis? Many tumor-associated environmental and biochemical factors are known to affect gene expression. For example, cytokine-producing inflammatory cells, such as macrophages, are a common feature of tumors but are rarely found in the corpus luteum when angiogenesis is maximal (Goede et al., 1999). Hypoxia, tumor-derived growth factors, and changes in blood flow can also affect gene expression. In this study, we set out to identify molecular markers that can differentiate pathological and physiological angiogenesis. In order to generate a model of physiological angiogenesis that could be readily controlled in a homogeneous genetic background, we took advantage of the fact that following 70% partial hepatectomy, the murine liver regenerates its mass over a period of 4 days, a process requiring angiogenesis (Michalopoulos and DeFrances, 1997; Drixler et al., 2002). We then developed methods to isolate ECs from isogenic normal adult livers, regenerating livers, and tumor-bearing livers. In an attempt to identify genes that are the most broadly expressed among tumors of various origins but are either absent or expressed at relatively low levels in all normal vessels, we also developed techniques to isolate ECs from multiple normal and tumor tissue types. We systematically compared gene expression profiles among the multiple samples by performing serial analysis of gene expression (SAGE) on the isolated ECs, an unbiased technique that can be used even when cell numbers are limited. These studies demonstrate the existence of multiple organ-specific endothelial transcripts as well as a number of genes that are selectively overexpressed in the vessels of tumors. Further analysis of the top cell surface tumor endothelial marker identified, CD276, revealed that, in humans, this cell surface receptor is overexpressed during pathological, but not physiological, angiogenesis. By unraveling the endothelial transcriptome, we have revealed the identity of several markers highly restricted to specific anatomical sites, including tumors, a finding which has significant implications for the development of the most selective vascular targeted therapies.

RESULTS

To begin to unravel the mouse endothelial transcriptome, we set out to develop a method that could be used to immunopurify ECs from a variety of tissue types. Immunopurification is difficult because the ECs are enmeshed in a complex tissue containing an extracellular matrix of variable composition and multiple nonendothelial cell types. Our initial attempts to purify ECs involved antibody recognition of CD31, the conventional cell surface marker used for affinity purification of mouse ECs. However, this marker proved to be suboptimal because of its cross-reactivity with hematopoietic cells (data not shown). Instead, we found that CD105 (endoglin) and/or VE-cadherin specifically localized to the ECs of normal and tumor tissues. For example, both anti-CD105 and anti-VE-cadherin antibodies specifically labeled ECs in heart, but CD105 was a more suitable marker in liver because antibodies against this surface receptor appeared to stain all the endothelium including sinusoidal ECs (Figures 1A and 1B) whereas anti-VE-cadherin antibodies did not (data not shown). The cell isolation strategy involved tissue dissociation, the removal of non-ECs, and, finally, the positive selection of ECs using magnetic beads coupled to either anti-VE-cadherin or anti-CD105 antibodies, the choice depending on the tissue being dissociated (see Experimental Procedures for details). To assess the purity of the isolated cells, we generated cDNA from either whole tissues or purified ECs and then performed quantitative reverse transcription polymerase chain reaction (QPCR). These studies revealed a marked enrichment of endothelial-specific genes such as VE-cadherin in each of the purified fractions compared to unfractionated whole tissues (Figure 1C) but little contamination by hematopoietic cells as judged by CD45 expression (B.S.C., unpublished data). Subsequent gene expression analysis (see below) confirmed the purity of the cells.

To begin to unravel the normal endothelial transcriptome, we performed longSAGE on ECs isolated from brain, heart, kidney, lung, muscle, spleen, and liver. These SAGE libraries utilize a 21 nucleotide "long tag" which facilitates the mapping of genes directly to genomic DNA even when EST or cDNA sequence is unavailable (Saha et al., 2002). In total, 700,189 tags were obtained from these 7 normal EC libraries (see Table S1 in the Supplemental Data available with this article online). An initial analysis of the SAGE data immediately revealed the expression of multiple transcripts that are known to be selectively expressed in endothelial cells including VE-cadherin, VEGFR2, von Willebrand Factor, CD31, CD105, and claudin 5. In contrast, markers of epithelial, hematopoietic, hepatocyte, and other potential contaminating cell types were absent or rare (Table S2).

To determine if we could identify organ-specific endothelial transcripts, we began by searching for brain endothelial markers (BEMs) defined as genes that were expressed 20-fold or higher in brain compared to all other normal endothelium (Table 1). The most abundant and differentially expressed gene identified was the brain glucose transporter *Slc2a1* (*Glut-1*), a blood-brain barrier (BBB) marker previously found to be expressed on the luminal surface of brain endothelium (Pardridge et al., 1990; Farrell and Pardridge, 1991). Importantly, 13 of the 27 BEMs (~50%) identified are predicted to reside at the cell surface, and at least 9 of these are transporters potentially involved in BBB function. Seven of the BEMs, including five cell surface transporters, were previously localized to brain endothelium by in situ staining, thus validating the SAGE data we obtained (for references see Table 1). Some of the cell surface transporters have also been detected in liver tissues where they appear to be expressed predominantly by hepatocytes or other non-ECs, consistent with their absence from our liver EC SAGE libraries (Gu et al., 2000; Konig et al., 2000; Mesli et al., 2004).

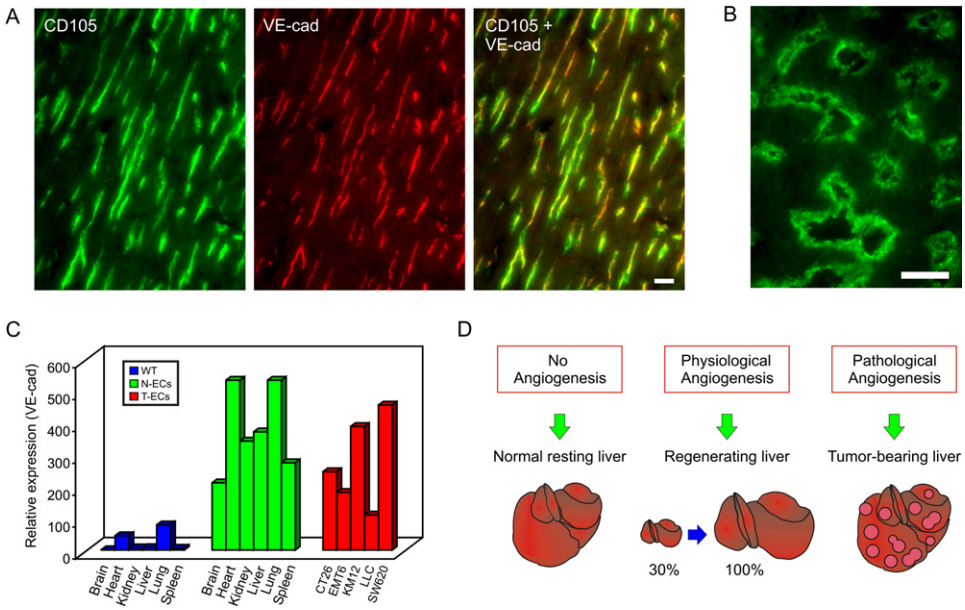

Figure 1. Purification of ECs from Normal and Malignant Tissues

(A) Immunofluorescence staining of heart tissue demonstrated colocalization of CD105 (green) with VE-cadherin (red) in the vessels. Scale bar, 20 μm.

(B) Immunofluorescence staining of liver tissue with CD105 (green). Scale bar, 20 μm.

(C) A QPCR analysis was used to assess the purity of the EC preparations. QPCR analysis was performed on cDNA generated directly from unfractionated normal whole tissues (WT) or from purified ECs isolated from normal tissues (N-ECs) or the tumors (T-ECs) indicated. The endothelial-specific transcript VE-cadherin was enriched 110- to 530-fold in the endothelial fractions. The modest level of VE-cadherin found in the unfractionated heart and lung sample is presumably due to a higher proportion of ECs in these tissues. In this experiment, gene expression was normalized to that of *Eif4h*, a gene found to be uniformly expressed in all cells as assessed by SAGE (Velculescu et al., 1999). Unfractionated brain was used to calibrate relative expression because this tissue had the lowest VE-cadherin expression levels.

(D) Model used to identify genes expressed during pathological, but not physiological, angiogenesis. ECs were isolated from normal resting livers, regenerating livers, or tumor bearing livers.

We also identified intracellular enzymes, such as glutathione-S-transferase α 4 (Gsta4), which could potentially be involved in protecting the brain from toxic chemicals that enter the blood.

We next identified genes that were overexpressed in liver endothelium, which we called liver endothelial markers (LEMs) (Table 1). The most highly expressed gene was deoxyribonuclease 1-like 3, a recently identified nuclease that may be involved with chromatin clearance from the circulation (Napirei et al., 2005). The best characterized gene identified was CD32, a low-affinity Fc γ-receptor that is a known marker of liver sinusoidal ECs (Muro et al., 1993). We also identified two lectin-like receptors, one of which was shown recently to be expressed predominantly by sinusoidal ECs of human liver and lymph node (Liu et al., 2004). Seven of the LEMs identified are predicted to reside at the cell surface, including three that have not yet been characterized. These results clearly highlight the complexity of blood vessels and demonstrate the existence of multiple organ-specific endothelial markers in different tissues.

Next, in order to identify genes that were elevated during physiological angiogenesis, ECs were isolated from liver 24, 48, or 72 hr following partial hepatectomy, the period during which EC division is thought to occur (Michalopoulos and DeFrances, 1997). In total, we isolated 395,234 SAGE tags from regenerating liver (Table S1). We then compared gene expression patterns of regenerating liver ECs with a combined set of EC libraries derived from all nonproliferating normal organs including resting liver (Figure 1D). This comparison revealed 12 genes that were overexpressed in regenerating liver ECs compared to nonangiogenic ECs (Table 2), which we refer to as angiogenesis endothelial markers (AEMs). At least seven of these genes are thought to be involved in regulating progression through the cell cycle, consistent with the fact that these ECs are dividing. For example, the most abundant AEM is an ubiquitin-conjugating enzyme, Ube2c. Its human counterpart, UBE2C (UBCH10), has been shown to be important for progression through the G1 phase of the cell cycle (Townsley et al., 1997; Rape and Kirschner, 2004). Protein regulator of cytokinesis 1 (PRC1) is a mitotic spindle-associated CDK substrate that is required for cytokinesis (Jiang et al., 1998). Ckap2 and Cks2 have also been shown to regulate cell cycle (Spruck et al., 2003; Tsuchihara et al., 2005), and DNA topoisomerase II-α (Top2a), thymidine kinase 1 (TK1), and the Ki-67 antigen have been used as markers of proliferating cells for more than two decades (Bradshaw, 1983; Gerdes et al., 1984; Sampson et al., 1992). We also identified one extracellular matrix glycoprotein, tenascin C, that has been frequently associated with angiogenesis of malignant tumors,

Table 1. SAGE Tags Elevated Specifically in Brain Endothelium or Liver Endothelium

	Brain	Heart	Kidney	Liver	Lung	Muscle	Spleen	Accession Numbers	Description[b]
BEMs									
1	754	8	1	2	1	12	4	NM_011400	GLUT-1[a] (Pardridge et al., 1990; Farrell and Pardridge, 1991)
2	157	0	0	0	0	1	0	NM_030687	Organic anion transporter 2[a] (Gao et al., 2000)
3	93	0	1	0	0	1	1	NM_008973	Pleiotrophin (Yeh et al., 1998)
4	32	0	0	0	0	0	0	NM_009728	ATPase, class V, type 10A[a]
5	40	0	0	0	1	0	0	NM_009402	Peptidoglycan recognition protein 1
6	26	0	0	0	0	0	0	NM_021471	Organic anion transp. 14[a] (Tohyama et al., 2004)
7	29	0	0	0	0	0	0	NM_008239	Forkhead box Q1
8	19	0	0	0	0	0	0	NM_031194	Organic anion transporter 3[a] (Mori et al., 2003; Ohtsuki et al., 2004)
9	73	0	0	0	3	0	0	NM_172479	SN2, Solute carrier family 38, member 5[a]
10	40	0	0	0	1	2	0	NM_172471	Interalpha (globulin) inhibitor H5
11	12	0	0	0	0	0	0	NM_010703	Lymphoid enhancer binding factor 1
12	23	0	0	0	0	0	1	NM_011404	Slc7a5 aa transporter[a] (Kageyama et al., 2000)
13	20	1	0	0	0	0	0	NM_023805	Solute carrier family 38, member 3[a]
14	17	0	0	0	0	0	0	NM_009574	Zinc finger protein of the cerebellum 2
15	81	6	0	0	1	3	0	NM_052994	Testican-2 (Schnepp et al., 2005)
16	26	0	1	0	1	1	0	NM_008256	3-HMG-CoA synthase 2
17	15	0	0	0	0	0	0	NM_028748	Progestin and adipoQ receptor family member V
18	68	0	1	2	1	0	1	AK172004	APC downregulated 1, Drapc1
19	13	0	0	1	0	0	0	NM_027096	Unknown[c], GDPD phosphodiesterase family
20	26	0	0	3	1	0	0	NM_029001	Unknown[c], putative transmembrane protein
21	19	1	0	0	0	1	0	NM_027299	DES2, lipid desaturase/ C4-hydroxylase
22	39	0	1	0	2	0	1	XM_486083	Unknown[c], kelch repeat and BTB (POZ) domain
23	46	2	1	0	1	1	0	NM_017405	Lipolysis stimulated receptor[a]
24	36	2	0	0	1	1	0	NM_010357	Glutathione S-transferase, alpha 4[a]
25	9	0	0	0	1	0	0	NM_013869	TNF receptor superfamily, member 19
26	17	1	0	0	0	1	0	NM_011532	T-box 1
27	6	0	0	0	1	0	0	XM_620023	Unknown[c], putative transmembrane protein
LEMs									
1	0	0	0	196	0	0	0	NM_007870	Deoxyribonuclease 1-like 3
2	0	0	0	58	0	0	3	NM_010959	LZP, oncoprotein induced transcript 3
3	0	0	0	16	0	0	0	NM_023438	Unknown[c], putative transmembrane protein

Table 1. *Continued*

	Brain	Heart	Kidney	Liver	Lung	Muscle	Spleen	Accession Numbers	Description[b]
4	1	0	0	123	0	0	6	AK150613	CD32 (Muro et al., 1993)
5	0	1	0	33	0	1	1	NM_033616	Unknown[c], putative G-protein coupled receptor
6	0	1	0	14	0	0	0	NM_019985	C-type lectin-like receptor 2
7	0	0	0	216	0	0	24	NM_029465	Clec4g (LSECtin) (Liu et al., 2004)
8	0	1	0	42	2	1	0	NM_018797	Plexin C1
9	0	1	0	9	0	0	0	NM_011719	Wnt9B
10	1	0	0	16	1	0	0	AK144596	Unknown
11	0	1	0	9	0	0	0	NM_008092	GATA-binding protein 4 (Dame et al., 2004)
12	0	0	0	10	1	2	0	AB049755	MBL-associated serine protease-3
13	0	0	0	5	0	0	1	NM_023132	Renin binding protein
14	0	0	0	16	1	2	1	NM_144830	Unknown[c], putative transmembrane protein
15	1	0	1	11	0	0	0	NM_011243	Retinoic acid receptor, beta

The 27 genes which displayed more than 20-fold expression in brain endothelium compared to the six other normal endothelial libraries shown are listed in descending order. Likewise, 14 genes were found to be expressed at levels 20-fold higher in liver endothelium compared to the other normal endothelial libraries. To calculate tag ratios, we assigned a value of 0.5 in cases where zero tags were observed. Tag numbers for each group were normalized to 100,000 transcripts except for kidney which was normalized to 30,000 tags due to the small number of tags obtained for that particular tissue (Table S1). The tag sequences corresponding to the genes shown can be found in Tables S4 and S5. Genbank accession numbers and a description of the gene product corresponding to each tag are given.

[a] Gene product has either a putative or established role in BBB function.

[b] Genes previously shown to be expressed in either brain or liver endothelium are followed by the associated references.

[c] Uncharacterized gene with structural domains indicated.

inflamed tissues, and healing wounds (Zagzag et al., 1996; Tanaka et al., 2004). The only AEM identified encoding a predicted cell surface product was integrin β3, a receptor that partners with integrin αv and is thought to regulate angiogenesis (Brooks et al., 1994).

In nonangiogenic endothelial libraries, SAGE tag counts for AEMs were often not observed, making the absolute level of expression of these transcripts in normal resting ECs unclear (Table 2). Therefore, to accurately determine relative expression levels and validate these genes using a more sensitive technique, we performed QPCR. In order to carefully evaluate gene expression kinetics following angiogenic stimulation, we evaluated expression of AEMs in ECs isolated at 6, 18, 40, 72, and 96 hr post-partial hepatectomy. For comparison, we also analyzed ECs isolated from each of seven normal tissues including brain, heart, intestine, kidney, liver, lung, and spleen (Table S3). All of the EC samples used for QPCR were derived from fresh EC isolations independent of those used to generate the initial SAGE libraries. The QPCR analysis confirmed that each of the AEMs were induced in the regenerating liver ECs with peak levels ranging from 15- to 100-fold over nonproliferating ECs (Figure 2A). All of the AEM genes identified were also overexpressed in tumor endothelial cells (see below), providing further evidence that expression of these genes is upregulated during angiogenesis. Although most of the genes displayed maximum mRNA expression at 72 hr, the genes encoding inhibin-β B and integrin β3 reached their peak expression levels by 6 hr. Such early endothelial response genes may be important upstream regulators of the angiogenic cascade.

Finally, in order to identify genes that were elevated only during pathological angiogenesis but not physiological angiogenesis in a controlled setting, we isolated ECs from tumors that were grown in the liver (Figure 1D). For these studies, we employed two metastatic colon cancer cell lines, CT26 and KM12SM, because this tumor type typically metastasizes to the liver. For comparison, we also isolated ECs from three different tumor types grown subcutaneously: SW620, LLC, and EMT6. We chose colon, lung, and mammary carcinomas because they represent three of the most prevalent tumor types in humans. SW620 and KM12SM are of human origin and were grown as tumor xenographs in immune-deficient mice, whereas CT26, EMT6, and LLC are of murine origin and were grown as syngeneic tumor graphs in immune-competent mice. A summary of the cell lines employed and the host strains used for endothelial purification can be found in Table S1.

In total, 592,610 SAGE tags were isolated from tumor ECs. Again, RT-PCR analysis and an evaluation of the SAGE tags for various cell-specific markers confirmed that the isolated cells were predominantly of endothelial origin (see Figure 1C and Table S2). A comparison of the

Table 2. Previously Characterized and Novel AEMs and TEMs

Normal Resting ECs							RL ECs			Tumor ECs						
Brain	Heart	Kidney	Liver	Lung	Muscle	Spleen	24 hr	48 hr	72 hr	CT26	EMT	KM	LLC	SW	Accession Numbers	Description[c]
AEMs																
0	0	0	0	0	0	0	0	10	14	5	3	4	9	0	NM_026785	Ube2c[a]
0	0	0	0	0	0	0	1	5	11	0	5	2	3	2	NM_026412	TRAF4af1
0	0	0	1	1	0	0	0	17	16	5	8	3	11	10	NM_011623	DNA topo IIα[a]
0	0	0	0	0	0	0	0	4	3	3	2	2	8	0	NM_001004140	Ckap2[a]
1	1	0	1	0	2	0	19	11	3	31	28	14	20	11	NM_008381	Inhibin beta-B
0	0	0	1	0	0	0	0	4	6	5	6	5	5	7	NM_025415	Cks2[a]
1	0	0	1	0	0	0	4	13	12	7	6	1	8	5	NM_009387	TK1[a]
0	0	0	0	1	2	0	0	2	6	5	14	16	24	12	NM_011607	Tenascin C
0	3	0	0	0	0	0	5	3	3	5	5	3	9	1	NM_024435	Neurotensin
0	0	0	1	1	0	0	0	5	10	5	3	4	10	0	NM_145150	Prc1[a]
0	0	0	0	1	1	2	0	11	12	7	7	2	5	4	XM_133912	Ki67 antigen[a]
0	1	0	1	0	1	1	3	5	3	17	10	6	4	9	NM_016780	Integrin-β3[b]
TEMs																
0	0	0	0	1	0	0	1	1	1	7	11	0	26	4	DQ832275	Vscp
0	1	0	0	0	0	0	0	1	0	1	6	3	10	16	DQ832276	CD276[b] (B7-H3)
0	0	0	0	1	0	0	0	0	1	6	4	5	9	12	DQ832277	ETSvg4 (Pea3)
0	1	0	0	0	0	0	0	0	0	8	2	1	26	3	DQ832278[d]	CD137[b] (4-1BB)
0	2	1	0	0	0	1	0	0	0	15	5	19	8	37	DQ832280	MiRP2[b]
0	0	0	0	0	0	0	0	0	0	3	5	0	2	1	NM_023137	Ubiquitin D (FAT10)
0	0	0	0	0	1	1	0	0	0	1	3	0	17	5	DQ832281	Doppel[b] (Prion-PLP)
0	0	1	0	1	0	0	0	0	0	0	6	2	7	7	DQ832282	Apelin
1	1	1	0	0	0	0	0	0	0	2	10	4	5	7	NM_008827	Plgf
0	1	0	0	1	0	0	0	0	0	14	1	1	5	0	DQ832283	Ptprn[b] (IA-2)
0	0	1	0	0	0	0	1	0	1	0	6	3	7	1	DQ832284	CD109[b]
1	0	0	0	0	0	0	2	1	0	10	1	1	5	1	DQ832285	Ankylosis[b]
0	0	1	0	1	0	0	1	0	0	3	2	8	1	5	NM_007739	Coll. VIII, α1

The top 12 AEM genes with the highest tag ratios are listed in descending order. Tags from regenerating liver (RL) ECs and tumor endothelial cells were combined and compared to the total tags derived from the seven normal endothelial libraries shown. In the bottom panel, the top 13 TEM genes with the highest tag ratios in tumor ECs compared to all nontumor endothelial libraries are shown. To calculate tag ratios, a value of 0.5 was assigned in cases where zero tags were observed. Tag numbers for each group were normalized to 100,000 transcripts except for kidney which was normalized to 30,000 tags due to the lower number of tags obtained for that particular tissue (Table S1). The gene product corresponding to each tag is given, followed by alternative names in parentheses. Genbank accession numbers and the gene name or symbol corresponding to each tag is given. Tag sequences corresponding to the genes shown can be found in Table S6 (AEMs) or Table S7 (TEMs).

[a] Genes encoding products thought to be important in cell-cycle control.

[b] Encodes known or predicted cell surface protein.

[c] Gene name is given followed by alternative names in parentheses.

[d] The Genbank accession number for the secreted variant sCD137 is DQ832279.

tumor EC libraries with normal ECs, including those from regenerating liver, revealed 13 genes that were that were at least 10-fold overexpressed in the endothelium of tumors (Table 2). Analysis of the cDNA and EST databases revealed multiple splice variants for many of these genes. In order to identify which sequences and splice variants were expressed in tumor endothelium we sequenced 10 of the 13 genes using tumor endothelial cDNA (for accession numbers, see Table 2). The most differentially expressed transcript was a previously uncharacterized gene that encodes a putative cytoplasmic protein containing an SH2 domain. This gene, which we called vascular SH2-containing protein (*Vscp*), was overexpressed 11- to 110-fold in tumor endothelium.

In total, 7 of the 12 genes were found to encode cell surface receptors. The most differentially expressed of these was *CD276*, followed by *CD137* (*Tnfrsf9, 4-1bb*). Sequencing of *CD137* revealed two products expressed in tumor ECs, one encoding the full-length membrane bound form, and another containing a variant that lacks the sixth exon encoding the transmembrane domain. This form, which we call sCD137, is presumably secreted and represents the mouse counterpart of the previously identified human sCD137 (Michel et al., 1998).

In order to validate the expression pattern of the TEMs identified by SAGE using a more sensitive technique, again we performed QPCR on our panel of normal and tumor ECs. Each of the newly identified tumor endothelial genes had a pattern of expression that was strikingly similar to that predicted by the SAGE data, with highest levels in tumor ECs and much lower levels in regenerating liver ECs similar to that observed in nonproliferating normal endothelium (Figure 2B). Most of the genes were overexpressed in the ECs of all of the tumors examined, although six of the genes (ankylosis, apelin, MiRP2, CD109, doppel, and ubiquitin D) appeared to be overexpressed in the vessels of only a subset of the tumor types. One of these, ubiquitin D, was only expressed in the vessels of mouse tumors (CT26, EMT6, and LLC), which we reasoned could potentially have been derived from contamination of the EC preparations with tumors cells. However, by RT-PCR analysis ubiquitin D mRNA was essentially undetectable in cultured tumor cell lines or tumor cell-enriched fractions prepared from tumor samples (Figure S1), suggesting that this was an unlikely explanation for the expression patterns observed.

To exclude the possibility that the differentially expressed transcripts were derived from other contaminating non-ECs, we performed mRNA in situ hybridization using a highly sensitive nonradioactive technique. First, we tested the top four brain endothelial markers and found each was localized to ECs throughout the brain whereas expression in liver was undetectable (Figure 3 and Table S8). Similarly, an analysis of five of the top LEMs revealed that each was readily detectable in liver endothelium but not brain endothelium. LEMs were expressed predominantly in the sinusoidal ECs with a pattern of staining similar to that of the endothelial control VEGFR2 (see Figure 3 and Table S8). However, LEM5, a previously uncharacterized putative G protein coupled receptor, was also found in the larger vessels of central veins, portal veins, and hepatic arteries.

We also evaluated 9 of the top tumor endothelial markers identified, and found each of them to be expressed in the ECs of various tumor types (Figures 4A and 4B). Importantly, for each of these TEMs, staining was undetectable in the endothelium of normal adult brain and liver tissues (Figure 4A and data not shown). However, mRNA in these control tissues was considered intact because LEMs, BEMs, and pan-endothelial controls such as *CD31* and *VEGFR2* were readily detected in these tissues. The positive signals observed for TEMs in tumor endothelium were considered specific because their patterns matched those observed with endothelial control probes and omission of the antisense riboprobes or substitution with a sense control resulted in a loss of signal in each case (data not shown). These data clearly demonstrate that these newly identified TEMs are expressed predominantly by tumor vessels.

The therapeutic potential of the genes identified will largely depend on whether or not the patterns of gene expression found in mice are recapitulated in humans and whether protein expression patterns follow mRNA expression patterns. One of the newly identified tumor endothelial markers, CD137, was recently found to be overexpressed in the vessels of a variety of human tumors and at sites of inflammation (Broll et al., 2001; Drenkard et al., 2007). Using antibodies against CD137, we were able to validate the overexpression of CD137 protein in lysates of human colorectal cancer compared to patient-matched normal colonic mucosa (see Figure S2). To begin addressing the expression pattern of additional TEMs in humans, we decided to focus on *CD276* because it was the most differentially expressed cell surface receptor identified by our SAGE analysis, and antibodies that specifically recognize human CD276 protein have recently become available. First, we generated riboprobes against human *CD276* and performed mRNA in situ hybridization on normal and malignant colorectal tissues. As shown in Figure 4C, *CD276* mRNA was most prominent in the tumor vessels, with a pattern of expression similar to that of the endothelial control VEGFR2. Unexpectedly, *CD276* expression was also detected in the tumor cells themselves, albeit at a lower level. In contrast, *CD276* expression was undetectable in normal colonic mucosa, and an analysis of the tumor margin showed a striking on/off pattern of staining at the tumor/normal border (Figure 4C, right panel).

Next, we sought to evaluate CD276 protein expression patterns using anti-CD276 antibodies. We began by assessing the overall level of CD276 in extracts taken from 12 normal and 12 malignant colorectal tissues, 10 of which were patient-matched. CD276 was clearly elevated in 11 of the 12 tumors, while the remaining matched normal/tumor pair (case P7) displayed unaltered expression (Figure 5A). We also evaluated CD276 expression levels in six lung tumors, and comparison with patient-matched controls revealed increased expression in each of the cases (Figure 5B). All tumor samples appeared to overexpress

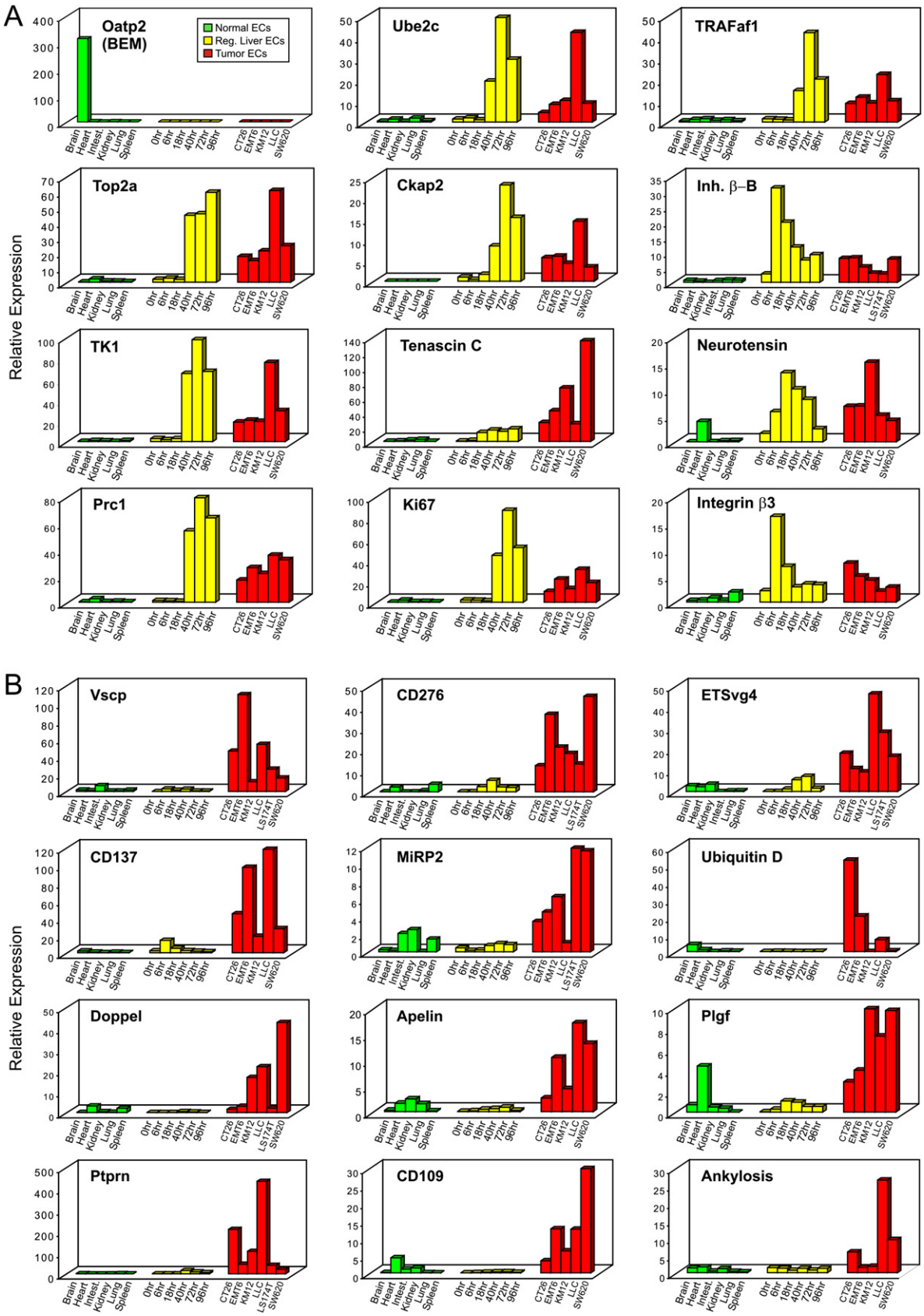
A
Oatp2 (BEM)
Normal ECs
Reg. Liver ECs
Tumor ECs
Ube2c
TRAFaf1
Top2a
Ckap2
Inh. β–B
TK1
Tenascin C
Neurotensin
Prc1
Ki67
Integrin β3
Relative Expression
B
Vscp
CD276
ETSvg4
CD137
MiRP2
Ubiquitin D
Doppel
Apelin
Plgf
Ptprn
CD109
Ankylosis
Relative Expression
Brain Heart Kidney Lung Spleen
0hr 6hr 18hr 40hr 72hr 96hr
CT26 EMT6 KM12 LLC LS174T SW620

the predominant 4-IgG form of CD276, as exogenous overexpression of this form in transfected 293 cells resulted in a product of similar size (Figure 5A).

To determine the cellular source of this upregulated protein and expand our analysis of tumors, we performed an immunohistochemical survey of various human tumor types including colon, lung, breast, esophageal, and bladder cancer. First, we analyzed paraffin sections taken from ten patient-matched samples of normal colonic mucosa and colorectal cancer or ten patient-matched samples of non-small-cell lung cancer along with adjacent normal lung tissue. All samples represented different cases than those used for immunoblotting. Staining with an anti-CD276 polyclonal antibody revealed a vessel-like pattern in all cases of human colorectal or lung cancer analyzed, but not in matched normal tissues (Figures 5C–5H and Table S9). Moreover, this vessel-like pattern of staining was also observed in each of a smaller number of breast, esophageal, and bladder cancers, but not in corresponding normal tissues (Figures 5I–5L). Similar expression patterns were observed using an independent monoclonal antibody (data not shown). Interestingly, again CD276 overexpression was frequently detected in the tumor cells while normal epithelium was uniformly negative. The highest tumor cell expression levels of CD276 were found in lung and breast cancer where they appeared to match that found in tumor endothelium (Figures 5F, 5G, and 5L).

To ensure that the antibodies were predominantly staining endothelial cells, colocalization studies were performed on six additional cases of normal or malignant colorectal tissues. In each case, we observed clear colocalization of CD276 protein with vWF, a classic endothelial marker (Figure 6A). Although the tumor vessels stained most intensely, again the tumor cells themselves appeared positive, while all cell types from normal colonic mucosa were negative. Next, we stained human corpus luteum to determine if the normal angiogenic vessels of this tissue express CD276. Unlike the vWF control, CD276 expression was not detected in these angiogenic vessels (Figure 6B). These studies demonstrate that CD276 is consistently overexpressed at the protein level in the blood vessels of various human cancers and may therefore represent a useful target for tumor-specific vascular targeting.

DISCUSSION

In order to gain a more comprehensive understanding of the endothelial transcriptome, we generated a gene expression database for ECs isolated from a panel of normal and malignant tissues. In total, we generated a data set of ~1.7 million endothelial SAGE tags, almost 10-fold deeper than our original endothelial data set (St. Croix et al., 2000). The large set of normal tissues proved valuable not only for identifying "tissue-specific" endothelial markers, but also for substantially limiting the number of tumor endothelial markers identified to those that were the least likely to share cross-reactivity with normal endothelium. Indeed, this point is readily apparent when the new SAGE libraries are specifically queried for TEMs which were identified in previous studies conducted on a single tissue type, i.e., normal and malignant human colorectal tissues (St. Croix et al., 2000). Four of the genes identified in those studies, *TEM1*, *TEM5*, *TEM7*, and *TEM8*, encode cell surface proteins and are of particular interest as potential vascular targets. The mouse ortholog of one of these genes, *Tem7*, did not appear to be overexpressed in the tumor endothelial libraries of our new SAGE database or when analyzed by QPCR (S.S. and B.S.C., unpublished data) consistent with previous mRNA in situ hybridization studies conducted on tumors in mice (Carson-Walter et al., 2001). Given that mice and humans diverged during evolution over 65 million years ago, it is not surprising that the cross-species expression patterns of certain genes do not always match one another. However, genes that are coordinately expressed have an obvious advantage for translational studies due to the immediate availability of appropriate models for preclinical testing of new therapeutic agents that target tumor vasculature. An analysis of the new SAGE data for *Tem1*, *Tem5*, and *Tem8* did reveal overexpression of these genes in mouse tumor endothelium. However, these 3 TEMs were excluded from the final list of angiogenic markers presented in this study because of similarly high expression in the ECs of one or more normal adult tissues. For example, *Tem1* expression was unexpectedly found in normal kidney ECs, *Tem5* in brain ECs, and *Tem8* in lung ECs (data not shown). Thus, identification of the most specific genes that are the least likely to share cross-reactivity with other tissues is greatly facilitated by the use of multiple normal tissues controls.

These studies also demonstrate that normal ECs from different anatomical sites can be readily distinguished based upon their unique gene expression signatures. Brain endothelium, for example, expressed a large number of unique cell surface transporters, several of which have already been implicated in BBB function. We also identified several previously uncharacterized cell surface transporters likely to have a role in maintaining the BBB. Liver endothelium also demonstrated a distinctive gene expression pattern. Such organ-specific endothelial markers hold much promise for the selective delivery of molecular medicine to targeted anatomical sites.

Figure 2. Gene Expression in Resting Normal ECs, Regenerating Liver ECs, and Tumor ECs

(A) Expression of AEMs is upregulated in regenerating liver ECs. Note the high expression levels of integrinß3 and inhibin-β B only 6 hr following partial hepatectomy. For comparison, expression patterns of a BEM (Organic-anion-transporter 2, *Oatp2*) are also shown in the upper left panel.

(B) Expression of TEMs is upregulated in tumor ECs. Note the low basal expression of these genes in regenerating liver ECs similar to that observed in ECs of normal resting tissues. Gene expression was evaluated by real-time QPCR and compared with that of *Srnp70*, a gene found to be expressed at nearly identical levels in all ECs by SAGE. For AEMs and TEMs, the results are expressed as a ratio between the gene of interest and *Srnp70* and are normalized to the average expression of all nonangiogenic normal ECs. For *Oatp2*, samples were normalized to the average expression in intestinal, heart and kidney ECs. For comparison, normal ECs from resting liver (time = 0 hr) were grouped with the regenerating liver ECs.

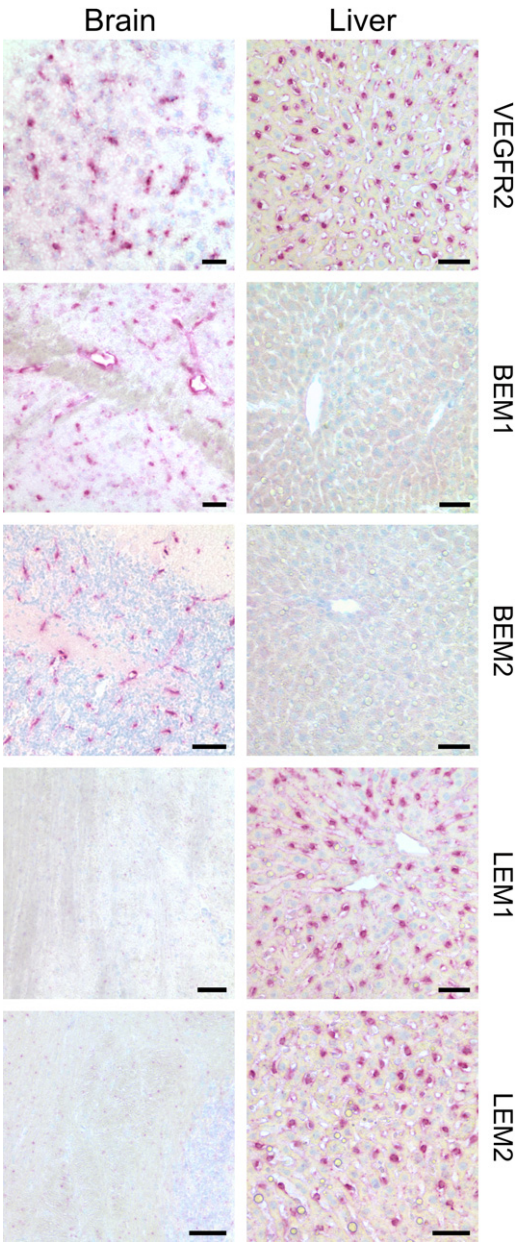

Figure 3. LEM and BEM Genes Identified by SAGE Are Expressed by ECs In Vivo

Localization of mRNA in ECs (red stain) is demonstrated for the brain endothelial markers GLUT-1 (BEM1) and organic anion transporter 2 (BEM2), and the liver endothelial markers deoxyribonuclease 1-like 3 (LEM1) and oncogene induced transcript 3 (LEM2). Note that the BEMs are selectively expressed in brain endothelium whereas the LEMs are selectively expressed in liver endothelium. The endothelial control probe, VEGFR2, stains both brain and liver endothelium. Staining of LEMs is most prominent in the sinusoidal endothelium, wherein the nuclear body appears to stain most intensely. A dilute counterstain was applied to the sections to highlight the lack of detectable expression in the non-ECs of the tissues. Scale bars, 50 μM

For decades, physiological and pathological angiogenesis have been known to be morphologically distinct (Sasaki et al., 1991). However, the extent of differential gene expression between these cellular states has remained elusive. Most of the well-studied molecules that are thought to regulate tumor angiogenesis such as VEGF, bFGF, the angiopoietins, and their receptors also regulate normal physiological angiogenesis. One notable exception is placental growth factor, one of the tumor-restricted endothelial markers identified in this study that was previously found to be important for pathological angiogenesis but not developmental angiogenesis using *Plgf*-knockout mice (Carmeliet et al., 2001). Although all genes expressed in tumor endothelium are expected to have some normal physiological function, they may not be expressed in all types of angiogenesis, or at the same developmental stage. Analogous to "oncofetal antigens" (Wepsic, 1983), some of the tumor endothelial markers we identified might normally be expressed during development but are turned off in the adult, except during pathological situations. One TEM that might have such an expression pattern is doppel, a cell surface prion-like receptor previously found to be expressed in mouse brain endothelium during development. Doppel expression levels peak with maximal vessel proliferation 1 week after birth, but are undetectable by 8 weeks (Robertson et al., 1985; Li et al., 2000). Consistent with these studies, we also failed to detect doppel in normal adult brain. Apelin is another TEM that was previously found to be expressed in developing vessels (Saint-Geniez et al., 2002; Kasai et al., 2004; Cox et al., 2006).

The most differentially expressed TEM identified by SAGE, *Vscp*, encodes a previously uncharacterized cytoplasmic SH2-containing protein. We identified the complete nucleotide sequence of *Vscp* and demonstrated the selective expression of this gene in tumor endothelium. However, evaluation of its potential as a therapeutic target of tumor endothelium will require further studies including the development of antibodies against the mouse and human VSCP protein. Seven of the remaining genes encode cell surface proteins, making them appealing potential targets for tumor-specific vascular therapy. Four of these genes are thought to be involved in regulating inflammatory or autoimmune responses. These include CD276, CD137, PTPRN, and CD109. The identification of immunoregulatory genes is not unexpected given that inflammatory cells are typically present in tumors. However, these genes were originally thought to be expressed only by the activated inflammatory cells themselves and not by tumor endothelium. One notable exception is CD137, which Broll and coworkers recently found, using immunohistochemical staining, to be highly expressed in the vessels of multiple different tumor types, while expression in normal vessels and inflammatory cells was undetectable (Broll et al., 2001). Although these results were initially unexpected by the authors performing that study, they are consistent with the expression patterns described here. Remarkably, antibodies against CD137 have been used to regress established tumors in a number of preclinical studies (Melero et al., 1997; Mittler et al., 2004). These responses were originally presumed to occur as a result of enhanced immunogenicity against the tumor cells. The

expression of cell surface CD137 in tumor vessels suggests that therapeutic CD137 antibodies may also mediate their effects in part by directly targeting the newly formed blood vessels. We found that tumor ECs overexpressed two forms of CD137, one that is membrane bound and one that is presumably secreted. Although the exact function of each of these forms is unclear, soluble CD137 is thought to be antagonistic to the costimulatory activity of membrane-bound CD137 on T cells. Thus, sCD137 secreted by tumor ECs may serve to reduce immune activity against tumors. Conversely, the antitumor effects observed using anti-CD137 antibodies could presumably be a result of enhanced immunogenicity toward tumor cells due to removal of antagonistic sCD137 produced by tumor vessels. Soluble CD137 has been found to be elevated in the sera of patients with rheumatoid arthritis, an autoimmune disease associated with aberrant angiogenesis (Michel et al., 1998). Our results suggest that sCD137 may also be elevated in solid tumors and may thus provide a useful surrogate marker of tumor angiogenesis.

As an initial step toward evaluating the therapeutic potential of additional endothelial targets in humans, we have begun by focusing on CD276, the most differentially expressed cell surface tumor-specific endothelial marker identified by SAGE in this study. CD276 is a recently identified member of the B7 family of immunoregulatory molecules that can be induced on T cells, B cells, and dendritic cells by a variety of inflammatory cytokines (Chapoval et al., 2001; Steinberger et al., 2004). Although the expression of CD276 on such cells could potentially complicate a vascular targeting approach, so far we have not been able to detect CD276 protein on inflammatory cells in tumors of mice or humans. In contrast, we did detect strong consistent staining of the tumor vasculature in colon, lung, breast, esophageal, and bladder cancers. Furthermore, in many of the tumors examined, we found CD276 protein was also overexpressed by the tumor cells themselves. In such cases, agents which target CD276 may target both the tumor and stromal compartments simultaneously, thus resulting in an enhanced therapeutic efficacy. That CD276 was undetectable in the angiogenic vessels of the corpus luteum suggests that this might be a particularly attractive candidate for future therapeutic studies aimed at selectively targeting the tumor vasculature.

EXPERIMENTAL PROCEDURES

Tumor Tissues, Cell Lines, and Animal Studies

Anonymized human tissue samples were provided by the Cooperative Human Tissue Network (CHTN), with approval from the NIH Office of Human Subject Research. CHTN is funded by the National Cancer Institute. EMT6 cells were a kind gift from Robert S. Kerbel, KM12SM cells were a kind gift from Isaiah J. Fidler, HCT116 cells were from the DCT tumor repository (NCI, Frederick), and LS174T, SW620, CT26, and LLC were from the American Type Culture Collection (Manassas, VA). All tumor cell lines were maintained in DMEM medium containing 10% fetal bovine serum. Tumors were made by inoculating 5×10^5 to 1×10^6 cells either subcutaneously or intrasplenically. To produce liver metastasis by intrasplenic injection, the spleen was exteriorized through a left lateral incision prior to tumor cell injection. The tumor cell suspension was allowed to enter the portal circulation over a period of 5 min, after which the spleen was removed. For 70% partial hepatectomy, the liver was exposed through a midline abdominal incision, and the two anterior lobes were exteriorized and the suspensory ligaments severed. The left lateral and caudal lobes were gently tied off prior to excision and placement of the remaining liver back into the peritoneal cavity. All animal experiments were performed in accordance with NCI-Frederick ACUC guidelines.

Endothelial Cell Isolations

Immediately following CO_2 euthanasia, normal or tumor tissues were resected, diced with a razor, and then digested in Hepatocyte Wash Buffer (Invitrogen, Carlsbad, CA) containing 2 mg/ml collagenase A (Roche, Indianapolis, IN) for 1 hr at 37°C. All subsequent steps were performed on ice or at 4°C. After filtering sequentially through 100 μm and 25 μm mesh, cells were pelleted and rinsed repeatedly with PBS containing 0.5% BSA (PBS/BSA) until the supernatant was transparent. To remove hematopoietic cells from the sample, we incubated cells with a mixture of streptavidin-linked dynabeads (Dynal, Lake Success, NY) that had been separately prebound to biotin anti-CD19, biotin anti-CD45 (BD Pharmingen, San Diego, CA), or biotin anti-F480 (Caltag Laboratories, Burlingame, CA) and then mixed at a 1:1:1 ratio. To prevent nonspecific binding of Fc-receptor containing cells in the positive selection, anti-CD16/32 antibodies (Fc Block; BD Pharmingen) were added to the cell suspension. For SAGE libraries, ECs from heart, kidney, intestine, liver, lung, KM12SM tumors, and LS174T tumors were labeled with biotinylated rat anti-mouse CD105 (eBioscience, San Diego, CA); to label ECs from spleen, CT26 tumors, or LLC tumors, biotinylated goat anti-mouse VE-cadherin (R&D Systems, Minneapolis, MN) was added, and to label ECs from brain, muscle, EMT6 tumors, and SW620, a mixture of both antibodies was added. The selection markers used to isolate ECs for QPCR can be found in Table S3. After rinsing five times with PBS/BSA, streptavidin-linked dynabeads were added to the cell suspension, rotated 5 min at 4°C, and diluted to 40 ml with PBS/BSA, and bead-bound cells were captured using a Dynal MPC-50 magnet. Captured ECs were rinsed five to ten times until only bead-bound cells were observed. Cells were resuspended in mRNA lysis/binding buffer for SAGE or mRNA extraction buffer for RT-PCR. After removing the beads, lysates were stored at −80°C until ready to use.

Construction of SAGE Libraries

LongSAGE libraries were constructed using the I-SAGE Long Kit (Invitrogen) and our previously established MicroSAGE protocol (for a detailed protocol see: http://www.sagenet.org/protocol/index.htm). Ditags were PCR amplified using biotinylated primers to facilitate efficient linker removal and Mme-I enzyme was purchased from New England Biolabs (Ipswich, MA). The endothelial SAGE data has been deposited into the SAGE Genie public database (http://cgap.nci.nih.gov/SAGE).

Quantitative PCR

mRNA was purified using the Quick Prep Micro mRNA purification kit (Amersham, Piscataway, NJ). Single-stranded cDNA was generated using the Superscript III first strand synthesis system (Invitrogen) following the manufacturer's directions. Quantitative PCR was performed with an MX4000 using Brilliant SYBR Green QPCR Master Mix, and threshold cycle numbers were obtained using MX4000 software v. 4.20 (Stratagene, La Jolla, CA). Primer sets for each sequence analyzed are included in Table S10. All primers were designed to span large introns thereby preventing potential amplification of contaminating genomic DNA. Primers were only used if they produced a single band of the expected size upon gel electrophoresis and failed to produce primer dimer products as assessed by gel electrophoresis and melting point analysis on the MX4000. Conditions for amplification were: one cycle of 95°C, 10 min followed by 40 cycles of 95°C, 20 s; 56°C, 30 s; and 72°C, 30 s. Quantitative PCRs were performed in duplicate, and threshold cycle numbers were averaged. Gene expression

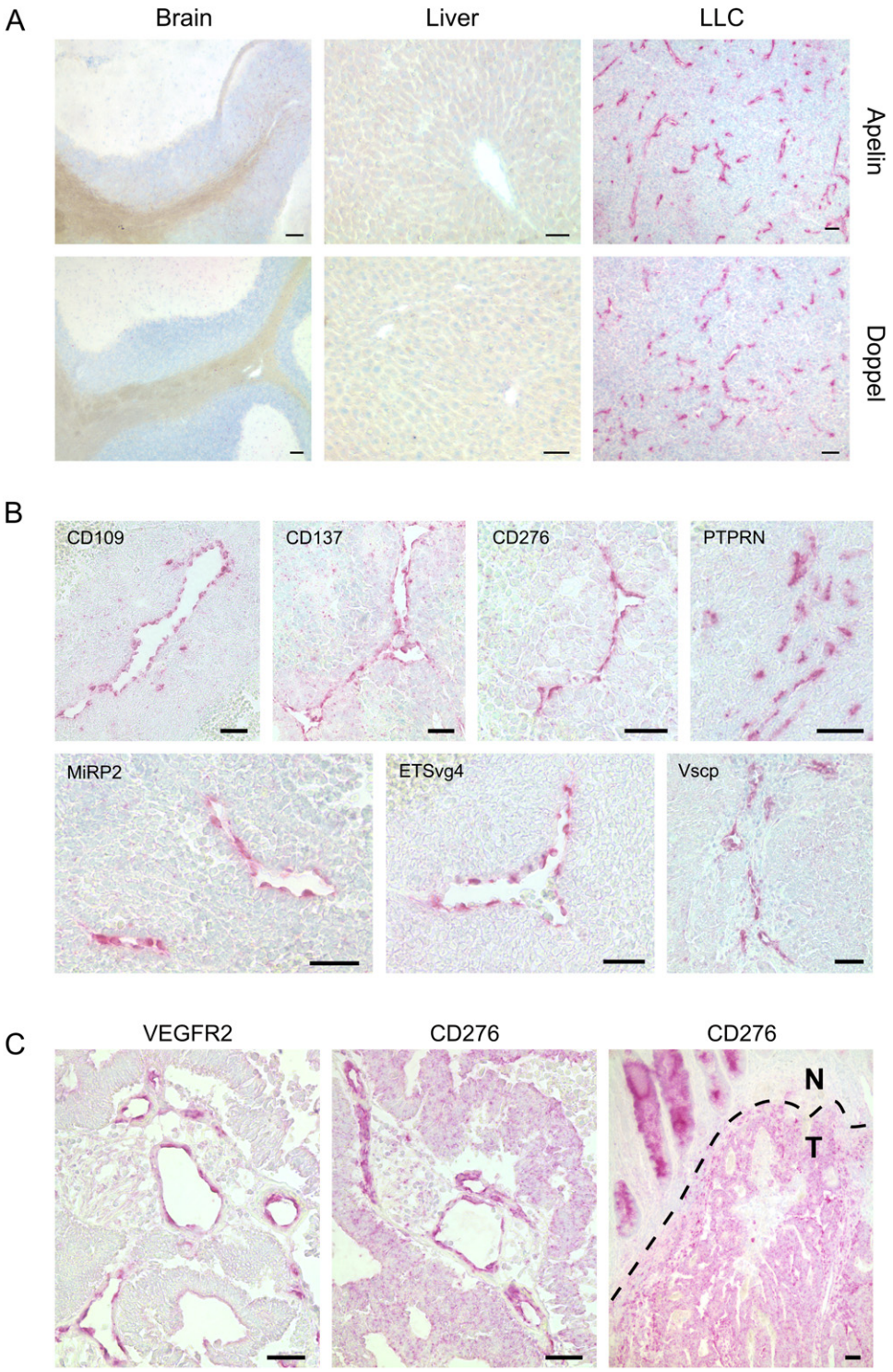

Figure 4. TEM Genes Identified by SAGE Are Expressed by Tumor ECs In Vivo

(A) Localization of mRNA in tumor ECs (red stain) was demonstrated by examining apelin and doppel in subcutaneous implanted LLC tumors. Note the lack of detectable expression in the normal brain and liver tissues of these representative TEMs.

(B) Localization of various TEMs in the tumor endothelium of mice. Depicted are *CD137* in a KM12SM tumor from the liver, *CD109* and *MiRP2* in SW620 subcutaneous tumors and *CD276*, *PTPRN*, *ETSvg4*, and *Vscp* in HCT116 subcutaneous tumors.

(C) *CD276* mRNA is expressed in the vessels of human colorectal cancer. In situ hybridization revealed that *CD276* mRNA is expressed predominantly in the vessels of human colorectal cancer (middle panel) with a pattern of staining similar to that of the control endothelial marker *VEGFR2* (left panel). Note that in the case of *CD276* the tumor cells also display positive staining, albeit less intense. At the margin between tumor (T) tissue and normal (N)

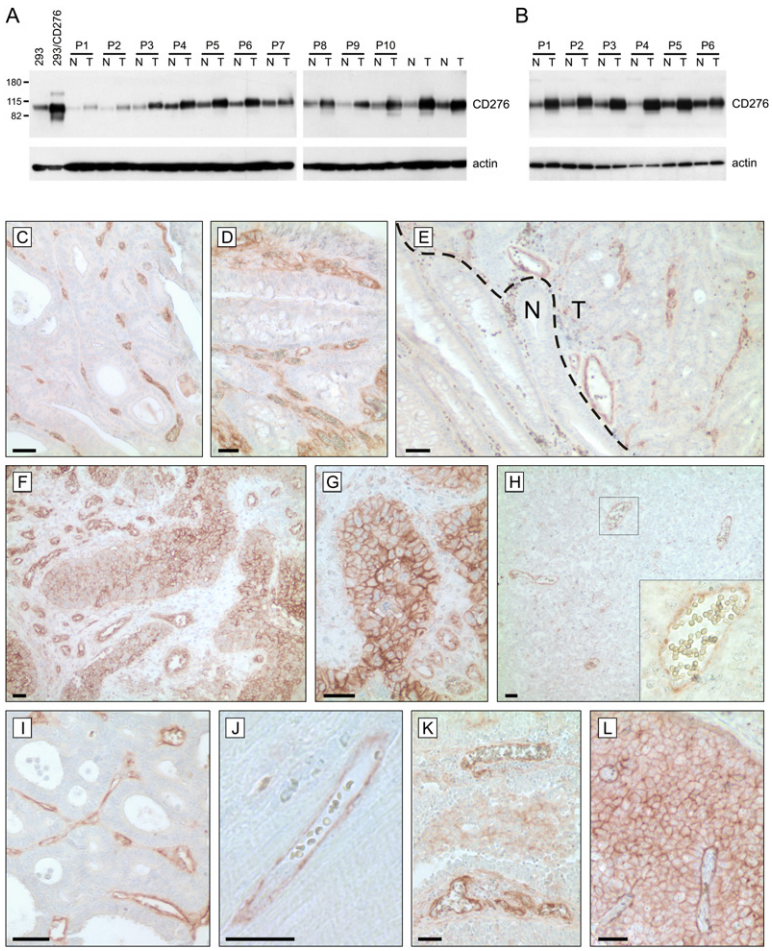

Figure 5. CD276 Protein Is Overexpressed in Human Tumors

(A) Immunoblotting with anti-CD276 monoclonal antibody revealed an upregulation of CD276 protein in colorectal tumors, T, compared to normal, N, colonic mucosa. Ten of the paired samples represent matched tissues taken from the same patient (P1–P10). CD276 protein migrates at a size similar to that observed in 293 cells transfected with the 4IgG-containing form of CD276 (293/CD276). The faint product present in 293 parent cells presumably represents low-level endogenous CD276 expression which can also be detected at the mRNA level in these cells by RT-PCR (data not shown).

(B) Immunoblotting with a CD276 monoclonal antibody revealed an upregulation of CD276 protein in lung tumors, T, compared to normal, N, adjacent lung tissue. The normal tissues in (A) and (B) were classified as normal based on gross morphology, but microscopic disease or inflammatory host cells may have contributed to the low level CD276 expression observed in these tissues.

(C–L) Immunohistochemical staining with a polyclonal CD276 antibody revealed a vessel-like pattern (brown stain) in colorectal cancer (C–E), non-small-cell lung cancer (F–H), esophageal cancer (I–J), bladder cancer (K), and breast cancer (L). At the tumor margin (E) CD276 staining was weak or undetectable in normal colonic mucosa, N, but strong in the vessels of the adjacent tumor region, T. Vessels from normal tissues that failed to stain for CD276 were immunoreactive on control serial sections stained for endothelial proteins such as vWF (data not shown). In some tumors, the vessels appeared to stain most prominently (C–E) and (H–K) whereas in others, both tumor cells and tumor vessels were strongly positive (F), (G), and (L). Note the strong cell surface staining pattern in the tumor epithelium under high power magnification (G). Many of the blood vessels were readily identified by the presence of blood cells in the lumen; for example see inset displaying higher power magnification of boxed region in (H). Sections were lightly counterstained with hematoxylin (blue stain). Scale bar, 50 μM.

was normalized to that of the 70 Kd U1 small nuclear ribonucleoprotein polypeptide A (*Srnp70*), a gene that is uniformly expressed in all ECs as assessed by SAGE. Relative expression was calculated using the equation $2^{(Rt-Et)}/2^{(Rn-En)}$ where Rt is the threshold cycle number observed in the experimental sample for Srnp70, Et is the threshold cycle number observed in the experimental sample for the gene of interest (GOI), Rn is the average threshold cycle number observed for Srnp70 in all the N-EC samples, and En is the average threshold cycle number observed for the GOI in all the N-EC samples.

In Situ Hybridization

Digoxigenin (DIG)-labeled antisense RNA probes were generated by PCR amplification of 500–600 bp products incorporating T7 promoters into the antisense primers. The primers used to generate riboprobes can be obtained from the authors upon request. In vitro transcription was performed with DIG RNA labeling reagents and T7 RNA polymerase according to the manufacturer's instructions (Roche). Tumors and normal tissues were dissected, embedded in OCT, frozen in a dry ice-methanol bath, and cryosectioned at 10 μm. All sections were immediately fixed with 4% paraformaldehyde, permeabilized with proteinase K, rinsed with 5X SSC, and incubated with RNA probes (100 ng/ml) diluted in ISH solution (Dako, Carpinteria, CA) overnight at 55°C. After washing three times with 2 × SSC, sections were incubated at 37°C with RNase Cocktail (Ambion, Austin, TX) diluted 1:200 in 2 × SSC. Slides were stringently washed twice in 2 × SSC/50% deionized formamide (American Bioanalytical, Natick, MA) and then once with 0.1 × SSC at 55°C. Before immunodetection, tissues were treated with peroxidase blocking reagent (Dako) and blocked with 1% blocking reagent (Roche) containing purified, nonspecific rabbit immunoglobulins (Dako). For signal amplification, a horseradish peroxidase-rabbit anti-DIG antibody (Dako) was used to catalyze the deposition of FITC-tyramide (GenPoint Fluorescein kit, Dako). Further amplification was achieved by adding horseradish peroxidase-rabbit anti-FITC (Dako), biotin-tyramide (GenPoint Kit, Dako), and then alkaline phosphatase rabbit anti-biotin (Dako). Signal was detected with the alkaline phosphatase substrate Fast Red TR/Napthol AS-MX (Sigma

colonic mucosa *CD276* staining abruptly ends (right panel). The red extracellular staining around the normal crypts represents nonspecific binding of the in situ hybridization reagents to the mucous (right panel) and is also present in control sections (data not shown). A dilute blue counterstain was applied to each of the sections. Scale bars, 50 μM.

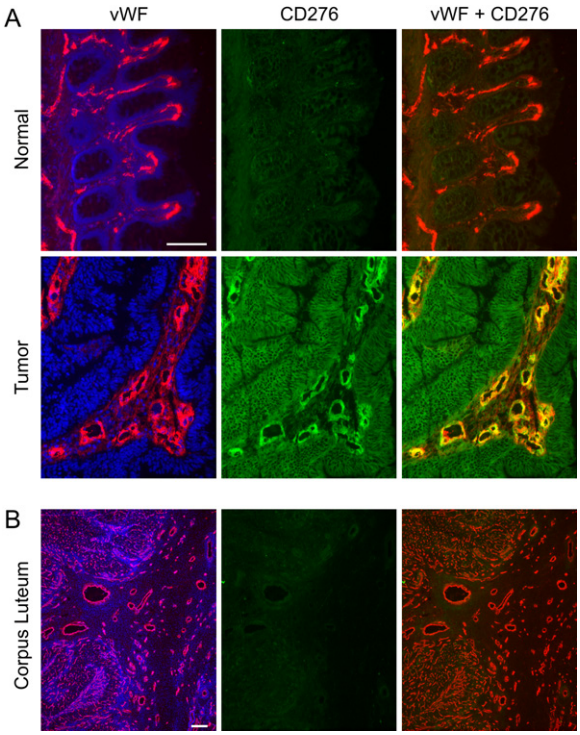

Figure 6. Immunofluorescence Staining Reveals Colocalization of CD276 with vWF in Human Colon Cancer

(A) CD276 (green) was expressed predominantly by the tumor vessels of the colorectal cancer, but was also expressed at a lower level by the tumor cells themselves. Expression of CD276 in normal colonic mucosa was undetectable (top middle panel). As a control, vessels were stained for vWF (Red) which colocalized with CD276 only in the tumor sample. Scale bar, 100 μm.

(B) CD276 expression was undetectable in the angiogenic vessels of the developing corpus luteum. Scale bar, 200 μm. Sections were counterstained with DAPI (blue), which is shown in the left panels to highlight the epithelial cells.

Chemical Co., St. Louis, MO). Cells were lightly counterstained with hematoxylin and mounted with Aqueous Mounting Medium (BioGenex, San Ramon, CA).

Immunohistochemistry

Paraffin sections were deparaffinized, incubated with proteinase K, heated at 95°C for 20 min in citrate buffer (pH6) (Invitrogen), and treated with peroxidase blocking reagent (Dako). Sections were incubated with a biotin-labeled polyclonal antibody against CD276 (R&D) followed by an HRP-conjugated anti-biotin antibody (Dako) and visualized by DAB (diaminobenzidine) staining. Sections were lightly counterstained with hematoxylin.

Immunoblotting

A CD276 expression vector was made by excising a human CD276 cDNA from an EST (accession number BC7472032) using the restriction enzymes EcoR1 and Not1 and cloning the fragment into the same sites of the expression vector pcDNA3.1(+) (Invitrogen). Sequencing of the CD276/pcDNA3 vector revealed that it contained a full length CD276 cDNA corresponding to transcript variant 1 (accession number NM_001024736). CD276/pcDNA3 was transfected into 293 cells using lipofectamine, and stable transfectants selected with Geneticin. To generate extracts for Immunoblotting, colorectal tissues stored at −80°C were thawed, diced with a razor, immediately homogenized in cold TNT buffer (50 mM Tris [pH 7.5], 75 mM NaCl, 1% triton X-100 containing a cocktail of protease inhibitors [Roche]), and clarified by centrifugation. Protein extracts from tissues or lysed 293 cells were separated by SDS-PAGE and transferred to a PDVF membrane (Millipore). Immunoblots were probed with a monoclonal anti-CD276 antibody (eBioscience) or an anti-actin antibody (Chemicon) followed by an HRP-conjugated anti-mouse secondary antibody (Jackson) and visualized using the ECL plus system (Amersham) according to the supplier's instructions. For CD137 detection, extracts were immunoprecipitated with goat anti-CD137 polyclonal antibodies (Sigma) and protein G and detected by Immunoblotting with the same antibody followed by an HRP-conjugated anti-goat F(ab')$_2$ antibody (Jackson).

Immunofluorescence

Dual-color immunofluorescence was performed on fresh-frozen sections fixed in Leukoperm (Serotec, Raleigh, NC). For CD105 detection, sections were stained with rat anti-mouse CD105 followed by FITC-linked goat-anti-rat (Jackson Immunoresearch Laboratories, West Grove, PA) and 488 goat anti-FITC (Invitrogen). VE-cadherin was detected using goat anti-mouse VE-cadherin followed by rhodamine-streptavidin (Vector Laboratories, Burlingame, CA). For dual CD276 and vWF immunofluorescence staining of human colorectal sections, we simultaneously stained tissues using a mouse anti-CD276 (R&D) monoclonal antibody, and a rabbit anti-vWF polyclonal antibody (DAKO). CD276 was detected with a FITC-conjugated goat anti-mouse antibody (Jackson Immunoresearch Laboratories) followed by a 488 goat-anti-FITC antibody (Invitrogen) and a 488 donkey anti-goat antibody (Invitrogen). vWF was detected using a biotin-linked donkey anti-rabbit antibody (Jackson Immunoresearch Laboratories) followed by rhodamine-streptavidin (Vector Laboratories, Burlingame, CA). Images were captured using a Nikon Eclipse E600 microscope.

Supplemental Data

The Supplemental Data include two supplemental figures and nine supplemental tables and can be found with this article online at http://www.cancercell.org/cgi/content/full/11/6/539/DC1/.

ACKNOWLEDGMENTS

We thank Dr. Karlyne Reilly and members of the Tumor Angiogenesis Section for their critical evaluation of the manuscript. This research was supported by the National Cancer Institute Department of Health and Human Services.

Received: June 30, 2006
Revised: March 23, 2007
Accepted: April 24, 2007
Published: June 11, 2007

REFERENCES

Bradshaw, H.D., Jr. (1983). Molecular cloning and cell cycle-specific regulation of a functional human thymidine kinase gene. Proc. Natl. Acad. Sci. USA *80*, 5588–5591.

Broll, K., Richter, G., Pauly, S., Hofstaedter, F., and Schwarz, H. (2001). CD137 expression in tumor vessel walls. High correlation with malignant tumors. Am. J. Clin. Pathol. *115*, 543–549.

Brooks, P.C., Clark, R.A., and Cheresh, D.A. (1994). Requirement of vascular integrin alpha v beta 3 for angiogenesis. Science *264*, 569–571.

Carmeliet, P., Moons, L., Luttun, A., Vincenti, V., Compernolle, V., De Mol, M., Wu, Y., Bono, F., Devy, L., Beck, H., et al. (2001). Synergism between vascular endothelial growth factor and placental growth factor contributes to angiogenesis and plasma extravasation in pathological conditions. Nat. Med. *7*, 575–583.

Carson-Walter, E.B., Watkins, D.N., Nanda, A., Vogelstein, B., Kinzler, K.W., and St. Croix, B. (2001). Cell surface tumor endothelial markers are conserved in mice and humans. Cancer Res. *61*, 6649–6655.

Chapoval, A.I., Ni, J., Lau, J.S., Wilcox, R.A., Flies, D.B., Liu, D., Dong, H., Sica, G.L., Zhu, G., Tamada, K., et al. (2001). B7–H3: A costimulatory molecule for T cell activation and IFN-gamma production. Nat. Immunol. *2*, 269–274.

Cox, C.M., D'Agostino, S.L., Miller, M.K., Heimark, R.L., and Krieg, P.A. (2006). Apelin, the ligand for the endothelial G-protein-coupled receptor, APJ, is a potent angiogenic factor required for normal vascular development of the frog embryo. Dev. Biol. *296*, 177–189.

Dame, C., Sola, M.C., Lim, K.C., Leach, K.M., Fandrey, J., Ma, Y., Knopfle, G., Engel, J.D., and Bungert, J. (2004). Hepatic erythropoietin gene regulation by GATA-4. J. Biol. Chem. *279*, 2955–2961.

Drenkard, D., Becke, F.M., Langstein, J., Spruss, T., Kunz-Schughart, L.A., Tan, T.E., Lim, Y.C., and Schwarz, H. (2007). CD137 is expressed on blood vessel walls at sites of inflammation and enhances monocyte migratory activity. FASEB J. *21*, 456–463.

Drixler, T.A., Vogten, M.J., Ritchie, E.D., van Vroonhoven, T.J., Gebbink, M.F., Voest, E.E., and Borel Rinkes, I.H. (2002). Liver regeneration is an angiogenesis- associated phenomenon. Ann. Surg. *236*, 703–711.

Farrell, C.L., and Pardridge, W.M. (1991). Blood-brain barrier glucose transporter is asymmetrically distributed on brain capillary endothelial lumenal and ablumenal membranes: An electron microscopic immunogold study. Proc. Natl. Acad. Sci. USA *88*, 5779–5783.

Ferrara, N., and Kerbel, R.S. (2005). Angiogenesis as a therapeutic target. Nature *438*, 967–974.

Gao, B., Hagenbuch, B., Kullak-Ublick, G.A., Benke, D., Aguzzi, A., and Meier, P.J. (2000). Organic anion-transporting polypeptides mediate transport of opioid peptides across blood-brain barrier. J. Pharmacol. Exp. Ther. *294*, 73–79.

Gerdes, J., Lemke, H., Baisch, H., Wacker, H.H., Schwab, U., and Stein, H. (1984). Cell cycle analysis of a cell proliferation-associated human nuclear antigen defined by the monoclonal antibody Ki-67. J. Immunol. *133*, 1710–1715.

Goede, V., Brogelli, L., Ziche, M., and Augustin, H.G. (1999). Induction of inflammatory angiogenesis by monocyte chemoattractant protein-1. Int. J. Cancer *82*, 765–770.

Gu, S., Roderick, H.L., Camacho, P., and Jiang, J.X. (2000). Identification and characterization of an amino acid transporter expressed differentially in liver. Proc. Natl. Acad. Sci. USA *97*, 3230–3235.

Jiang, W., Jimenez, G., Wells, N.J., Hope, T.J., Wahl, G.M., Hunter, T., and Fukunaga, R. (1998). PRC1: A human mitotic spindle-associated CDK substrate protein required for cytokinesis. Mol. Cell *2*, 877–885.

Kageyama, T., Nakamura, M., Matsuo, A., Yamasaki, Y., Takakura, Y., Hashida, M., Kanai, Y., Naito, M., Tsuruo, T., Minato, N., et al. (2000). The 4F2hc/LAT1 complex transports L-DOPA across the blood-brain barrier. Brain Res. *879*, 115–121.

Kasai, A., Shintani, N., Oda, M., Kakuda, M., Hashimoto, H., Matsuda, T., Hinuma, S., and Baba, A. (2004). Apelin is a novel angiogenic factor in retinal endothelial cells. Biochem. Biophys. Res. Commun. *325*, 395–400.

Kerbel, R., and Folkman, J. (2002). Clinical translation of angiogenesis inhibitors. Nat. Rev. Cancer *2*, 727–739.

Konig, J., Cui, Y., Nies, A.T., and Keppler, D. (2000). A novel human organic anion transporting polypeptide localized to the basolateral hepatocyte membrane. Am. J. Physiol. Gastrointest. Liver Physiol. *278*, G156–G164.

Li, A., Sakaguchi, S., Shigematsu, K., Atarashi, R., Roy, B.C., Nakaoke, R., Arima, K., Okimura, N., Kopacek, J., and Katamine, S. (2000). Physiological expression of the gene for PrP-like protein, PrPLP/Dpl, by brain endothelial cells and its ectopic expression in neurons of PrP-deficient mice ataxic due to Purkinje cell degeneration. Am. J. Pathol. *157*, 1447–1452.

Liu, W., Tang, L., Zhang, G., Wei, H., Cui, Y., Guo, L., Gou, Z., Chen, X., Jiang, D., Zhu, Y., et al. (2004). Characterization of a novel C-type lectin-like gene, LSECtin: Demonstration of carbohydrate binding and expression in sinusoidal endothelial cells of liver and lymph node. J. Biol. Chem. *279*, 18748–18758.

Melero, I., Shuford, W.W., Newby, S.A., Aruffo, A., Ledbetter, J.A., Hellstrom, K.E., Mittler, R.S., and Chen, L. (1997). Monoclonal antibodies against the 4–1BB T-cell activation molecule eradicate established tumors. Nat. Med. *3*, 682–685.

Mesli, S., Javorschi, S., Berard, A.M., Landry, M., Priddle, H., Kivlichan, D., Smith, A.J., Yen, F.T., Bihain, B.E., and Darmon, M. (2004). Distribution of the lipolysis stimulated receptor in adult and embryonic murine tissues and lethality of LSR−/− embryos at 12.5 to 14.5 days of gestation. Eur. J. Biochem. *271*, 3103–3114.

Michalopoulos, G.K., and DeFrances, M.C. (1997). Liver regeneration. Science *276*, 60–66.

Michel, J., Langstein, J., Hofstadter, F., and Schwarz, H. (1998). A soluble form of CD137 (ILA/4–1BB), a member of the TNF receptor family, is released by activated lymphocytes and is detectable in sera of patients with rheumatoid arthritis. Eur. J. Immunol. *28*, 290–295.

Mittler, R.S., Foell, J., McCausland, M., Strahotin, S., Niu, L., Bapat, A., and Hewes, L.B. (2004). Anti-CD137 antibodies in the treatment of autoimmune disease and cancer. Immunol. Res. *29*, 197–208.

Mori, S., Takanaga, H., Ohtsuki, S., Deguchi, T., Kang, Y.S., Hosoya, K., and Terasaki, T. (2003). Rat organic anion transporter 3 (rOAT3) is responsible for brain-to-blood efflux of homovanillic acid at the abluminal membrane of brain capillary endothelial cells. J. Cereb. Blood Flow Metab. *23*, 432–440.

Muro, H., Shirasawa, H., Kosugi, I., and Nakamura, S. (1993). Defect of Fc receptors and phenotypical changes in sinusoidal endothelial cells in human liver cirrhosis. Am. J. Pathol. *143*, 105–120.

Nanda, A., Carson-Walter, E.B., Seaman, S., Barber, T.D., Stampfl, J., Singh, S., Vogelstein, B., Kinzler, K.W., and St. Croix, B. (2004). TEM8 interacts with the cleaved C5 domain of collagen alpha 3(VI). Cancer Res. *64*, 817–820.

Napirei, M., Wulf, S., Eulitz, D., Mannherz, H.G., and Kloeckl, T. (2005). Comparative characterization of rat deoxyribonuclease 1 (Dnase1) and murine deoxyribonuclease 1-like 3 (Dnase1l3). Biochem. J. *389*, 355–364.

Ohtsuki, S., Kikkawa, T., Mori, S., Hori, S., Takanaga, H., Otagiri, M., and Terasaki, T. (2004). Mouse reduced in osteosclerosis transporter functions as an organic anion transporter 3 and is localized at abluminal membrane of blood-brain barrier. J. Pharmacol. Exp. Ther. *309*, 1273–1281.

Pardridge, W.M., Boado, R.J., and Farrell, C.R. (1990). Brain-type glucose transporter (GLUT-1) is selectively localized to the blood-brain barrier. Studies with quantitative western blotting and in situ hybridization. J. Biol. Chem. *265*, 18035–18040.

Rape, M., and Kirschner, M.W. (2004). Autonomous regulation of the anaphase-promoting complex couples mitosis to S-phase entry. Nature *432*, 588–595.

Robertson, P.L., Du Bois, M., Bowman, P.D., and Goldstein, G.W. (1985). Angiogenesis in developing rat brain: An in vivo and in vitro study. Brain Res. *355*, 219–223.

Saha, S., Sparks, A.B., Rago, C., Akmaev, V., Wang, C.J., Vogelstein, B., Kinzler, K.W., and Velculescu, V.E. (2002). Using the transcriptome to annotate the genome. Nat. Biotechnol. *20*, 508–512.

Saint-Geniez, M., Masri, B., Malecaze, F., Knibiehler, B., and Audigier, Y. (2002). Expression of the murine msr/apj receptor and its ligand apelin is upregulated during formation of the retinal vessels. Mech. Dev. *110*, 183–186.

Sampson, S.A., Kreipe, H., Gillett, C.E., Smith, P., Chaudary, M.A., Khan, A., Wicks, K., Parwaresch, R., and Barnes, D.M. (1992). KiS1–a novel monoclonal antibody which recognizes proliferating cells: Evaluation of its relationship to prognosis in mammary carcinoma. J. Pathol. *168*, 179–185.

Sasaki, K., Kiuchi, Y., Sato, Y., and Yamamori, S. (1991). Morphological analysis of neovascularization at early stages of rat splenic autografts in comparison with tumor angiogenesis. Cell Tissue Res. *265*, 503–510.

Schnepp, A., Komp Lindgren, P., Hulsmann, H., Kroger, S., Paulsson, M., and Hartmann, U. (2005). Mouse testican-2. Expression, glycosylation, and effects on neurite outgrowth. J. Biol. Chem. *280*, 11274–11280.

Spruck, C.H., de Miguel, M.P., Smith, A.P., Ryan, A., Stein, P., Schultz, R.M., Lincoln, A.J., Donovan, P.J., and Reed, S.I. (2003). Requirement of Cks2 for the first metaphase/anaphase transition of mammalian meiosis. Science *300*, 647–650.

St. Croix, B., Rago, C., Velculescu, V., Traverso, G., Romans, K.E., Montgomery, E., Lal, A., Riggins, G.J., Lengauer, C., Vogelstein, B., et al. (2000). Genes expressed in human tumor endothelium. Science *289*, 1197–1202.

Steinberger, P., Majdic, O., Derdak, S.V., Pfistershammer, K., Kirchberger, S., Klauser, C., Zlabinger, G., Pickl, W.F., Stockl, J., and Knapp, W. (2004). Molecular characterization of human 4Ig-B7–H3, a member of the B7 family with four Ig-like domains. J. Immunol. *172*, 2352–2359.

Tanaka, K., Hiraiwa, N., Hashimoto, H., Yamazaki, Y., and Kusakabe, M. (2004). Tenascin-C regulates angiogenesis in tumor through the regulation of vascular endothelial growth factor expression. Int. J. Cancer *108*, 31–40.

Tohyama, K., Kusuhara, H., and Sugiyama, Y. (2004). Involvement of multispecific organic anion transporter, Oatp14 (Slc21a14), in the transport of thyroxine across the blood-brain barrier. Endocrinology *145*, 4384–4391.

Townsley, F.M., Aristarkhov, A., Beck, S., Hershko, A., and Ruderman, J.V. (1997). Dominant-negative cyclin-selective ubiquitin carrier protein E2-C/UbcH10 blocks cells in metaphase. Proc. Natl. Acad. Sci. USA *94*, 2362–2367.

Tsuchihara, K., Lapin, V., Bakal, C., Okada, H., Brown, L., Hirota-Tsuchihara, M., Zaugg, K., Ho, A., Itie-Youten, A., Harris-Brandts, M., et al. (2005). Ckap2 regulates aneuploidy, cell cycling, and cell death in a p53-dependent manner. Cancer Res. *65*, 6685–6691.

Velculescu, V.E., Madden, S.L., Zhang, L., Lash, A.E., Yu, J., Rago, C., Lal, A., Wang, C.J., Beaudry, G.A., Ciriello, K.M., et al. (1999). Analysis of human transcriptomes. Nat. Genet. *23*, 387–388.

Wepsic, H.T. (1983). Overview of oncofetal antigens in cancer. Ann. Clin. Lab. Sci. *13*, 261–266.

Yeh, H.J., He, Y.Y., Xu, J., Hsu, C.Y., and Deuel, T.F. (1998). Upregulation of pleiotrophin gene expression in developing microvasculature, macrophages, and astrocytes after acute ischemic brain injury. J. Neurosci. *18*, 3699–3707.

Zagzag, D., Friedlander, D.R., Dosik, J., Chikramane, S., Chan, W., Greco, M.A., Allen, J.C., Dorovini-Zis, K., and Grumet, M. (1996). Tenascin-C expression by angiogenic vessels in human astrocytomas and by human brain endothelial cells in vitro. Cancer Res. *56*, 182–189.